Synthesis, characterization, and manipulation of dendrimer-stabilized iron sulfide nanoparticles

Xiangyang Shi[1]**, Kai Sun**[2]**, Lajos P Balogh**[1] **and James R Baker Jr**[1]

[1] Michigan Nanotechnology Institute for Medicine and Biological Sciences,
University of Michigan, Ann Arbor, MI 48109-0533, USA
[2] Electron Microbeam Analysis Laboratory, University of Michigan, Ann Arbor,
MI 48109-2143, USA

E-mail: jbakerjr@umich.edu

Abstract
FeS nanoparticles (NPs) were synthesized using ethylenediamine core
poly(amidoamine) (PAMAM) dendrimers of generation 4 terminated with
amino (G4·NH$_2$), hydroxyl (G4·NGlyOH), and carboxyl (G4·SAH) groups,
respectively, as stabilizers. These dendrimer-stabilized FeS NPs (FeS
DSNPs) were characterized by ultraviolet–visible (UV–vis) spectrometry,
zeta-potential measurements, and transmission electron microscopy (TEM).
Deposition of FeS NPs onto mesoporous silica gel microparticles was
attempted using two approaches: (A) direct coating of {FeS–G4·NH$_2$}
DSNPs onto silica particles; and (B) using G4·NH$_2$-coated silica particles to
incorporate Fe^{2+} ions for the subsequent formation of FeS NPs. Scanning
electron microscopy (SEM) studies show that approach (B) was much more
efficient in the incorporation of FeS NPs than approach (A). Such preparation
and manipulation of FeS DSNPs provides a unique strategy for fabricating
various reactive nanoplatforms for environmental remediation applications.

1. Introduction

Nanoparticles (NPs), because of their size, unusual crystal shapes, and lattice orders, have received great scientific and technological interest in environmental remediation [1]. FeS-based minerals are a particularly important, viable reactive medium, which displays higher reactivity than zero-valent iron in the reductive dechlorination of chlorinated hydrocarbons [2]. Nano-sized FeS particles are expected to exhibit much higher reactivity because of their larger surface area than bulk particles. Various methods have been employed to produce FeS NPs, including high-energy mechanical milling combined with mechanochemical processing [3], sulfate-reducing bacteria-assisted production [4–6], carbon dioxide laser pyrolysis of iron complexes [7], and reverse micelle [8, 9] or polymer-stabilized wet-chemical synthesis [10]. However, the preparation of functionalized FeS NPs using different methods still remains a great challenge.

One of the unique approaches used to prepare inorganic NPs is through the use of poly(amidoamine) (PAMAM) dendrimers as templates or stabilizers [11–19]. Dendrimers are a novel class of polymers with a close to spherical shape and a narrow size distribution [20] that can be used as templates or stabilizers to form relatively monodispersed organic/inorganic hybrid NPs. It has been demonstrated that copper sulfide [21] and cadmium sulfide [22, 23] can be formed using PAMAM dendrimers as templates or stabilizers. The crucial role played by dendrimers to synthesize dendrimer-stabilized NPs is that metal ions are usually complexed with dendrimer ligands (e.g. interior tertiary amines, terminal functional groups) through coordination, electrostatic interaction, etc, followed by reduction or other reactions to form inorganic NPs stabilized by dendrimers. To our knowledge, there is no reported literature describing the use of PAMAM dendrimers as stabilizers to synthesize FeS NPs. It is known that functionalized dendrimer derivatives can be used as templates or stabilizers to synthesize metal NPs with desired functionalities [24–26]. For instance, Au NPs prepared using hydrophobically modified PAMAM dendrimers as templates can be dissolved into various organic solvents [25]. It is

anticipated that the surface potential and optical absorption behaviour of FeS NPs can be varied by preparing them using different surface-functionalized PAMAM dendrimers as stabilizers. Compared with linear polymers with similar side chain groups that are used to synthesize NPs, the major advantages of using dendrimers are that the highly branched structure of dendrimers can significantly limit the overgrowth of NPs during their nucleation process, and the monodispersity of dendrimers can facilitate the formation of relatively monodispersed NPs.

For environmental applications, NPs are often embedded into thin polymer films or coated onto microparticle surfaces in order for them to be reusable and recyclable. Among many approaches used to prepare nanoparticulate thin films, electrostatic layer-by-layer (LbL) assembly using oppositely charged polymers and NPs has recently received great attention because the thickness and composition of the films can be controlled by changing the number of alternating deposition cycles and the charged species, respectively, through this unique approach [27]. Another advantage of the LbL self-assembly method is that the films can be formed not only onto planar substrates but also onto three-dimensional colloidal particles [28, 29], providing a facile way for one to manipulate NPs in planar polymer thin films or onto colloidal supports. The polymer films fabricated through electrostatic LbL self-assembly can also be used as a nanoreactor system for the *in situ* synthesis of NPs inside the films [30]. We expect that FeS NPs can be formed through the polymer film nanoreactor system and the dendrimer-stabilized FeS NPs (FeS DSNPs) can be self-assembled onto colloidal microparticles through electrostatic interaction for environmental remediation applications.

In this study, FeS NPs were synthesized using ethylene-diamine core generation 4 PAMAM dendrimers with amine (G4·NH$_2$), hydroxyl (G4·NGlyOH), and carboxyl (G4·SAH) terminal groups, respectively, as stabilizers. These FeS DSNPs were characterized by UV–vis spectroscopy, zeta-potential measurements, and transmission electron microscopy (TEM). Deposition of FeS DSNPs onto mesoporous silica gel microparticles was attempted using two approaches: (A) direct coating of {FeS–G4·NH$_2$} DSNPs onto negatively charged silica microparticles through electrostatic assembly; and (B) first coating G4·NH$_2$ dendrimers onto silica microparticles, followed by incorporating Fe^{2+} ions in the PAMAM mono-layer for subsequent formation of FeS NPs. The coating of FeS NPs onto colloidal silica microparticles was character-ized by zeta-potential measurements and scanning electron mi-croscopy (SEM) that combines with an x-ray energy dispersive spectroscopy (EDS) system for compositional analysis. The ef-ficiency of the deposition of FeS NPs onto silica microparticles using the above two approaches was compared. The synthesis and manipulation of FeS NPs onto colloidal microparticles pro-vides variable formulations for one to design different valuable nanoplatforms for environmental remediation applications.

2. Materials and methods

2.1. Materials

G4·NH$_2$, G4·NGlyOH, and G4·SAH were prepared and characterized in our previous report [31]. Fe(NH$_4$)$_2$(SO$_4$)$_2$, FeCl$_2$, NaCl, and Na$_2$S·9H$_2$O of reagent grade were purchased from Aldrich. Mesoporous Silica Gel60 (pore size = 6 nm, particle size = 40–63 μm) was purchased from Merck. Water used in all the experiments was pretreated by a Milli-Q Plus 185 water purification system (Millipore, Bedford, MA, USA) with a resistivity higher than 18 MΩ cm and bubbled with N$_2$ for 1 h before the preparation of all the solutions of dendrimers, iron salts, and sodium sulfide salts.

2.2. Preparation of FeS DSNPs in aqueous solutions

Under the protection of N$_2$ atmosphere, into a 20 ml vial was added a 5 ml dendrimer solution (concentration = 1.2×10^{-4} M), followed by the addition of a 0.25 ml FeCl$_2$ or Fe(NH$_4$)$_2$(SO$_4$)$_2$ solution (concentration = 2×10^{-3} M) under vigorous stirring. After 10 min, an equal volume of Na$_2$S solution with the same concentration of FeCl$_2$ or Fe(NH$_4$)$_2$(SO$_4$)$_2$ was added into the vial under vigorous stirring. The reaction was stopped after 30 min. Parallel samples were prepared and stored into 2 ml sealed ampoules. The stability of the FeS DSNP solutions in sealed ampoules was studied using UV–vis spectrometry under different conditions ('dark' at room temperature, 'bright' at room temperature, 'dark' at 4 °C, and 'bright' at 4 °C). Note that 'dark' and 'bright' in this context mean that the sealed ampoules are covered with or without aluminium foils, respectively.

2.3. Deposition of FeS DSNPs onto mesoporous silica gel microparticles

Two approaches were undertaken to coat FeS NPs onto silica microparticles. Approach (A): preformed {FeS–G4·NH$_2$} DSNP solution prepared using FeCl$_2$ salt ([FeS] = 1.7×10^{-4} M, 1 ml) was added into a 0.5 ml silica gel particle suspension (containing 10 mg silica gel particles) for 2 h under stirring. The unadsorbed FeS DSNPs were removed by three cycles of centrifugation (3000 rpm × 7 min)/washing/dispersion steps. Approach (B): silica particles were first coated with a monolayer of G4·NH$_2$ dendrimers by exposing 10 mg silica particles to 1 ml G4·NH$_2$ dendrimer solution (concentration: 2.4×10^{-4} M) for 2 h while stirring. The unadsorbed G4·NH$_2$ dendrimers were removed through three repeated cycles of centrifugation/washing/dispersion in water. Then, Fe^{2+} ions (FeCl$_2$ salt, concentration 2×10^{-3} M) were complexed with the amine groups of the dendrimers for subsequent reaction with Na$_2$S solution (concentration 2×10^{-3} M) to form FeS NP-loaded silica particles. Each step of the modification of silica particles was followed by three cycles of centrifugation/washing/dispersion in water. Note that each dispersion step was performed by sonicating the particle suspension for 30 s to 1 min.

2.4. Instrumentation

UV–vis spectrometry was performed using a Perkin Elmer Lambda 20 UV–vis spectrometer. The formation of FeS DSNPs was characterized by UV–vis spectrometry. TEM was performed using a JEOL 2010F analytical electron microscope with an operating voltage of 200 kV. 5–10 μl of FeS DSNP solutions were dropped onto carbon-coated copper grids and

air-dried before TEM measurements. Selected-area electron diffraction (SAED) was used to characterize the crystalline structures of the FeS DSNPs. An ultra-thin Be window Si–Li x-ray EDS detector with an active area of 30 mm^2 (EDAX, Draper, UT, USA) was employed for compositional analysis of the NPs. EDAX Genesis software was used for EDS data collection and processing. Zeta-potential measurements were performed using a PSS/NICOMP 380 ZLS particle sizing system (Santa Barbara, CA, USA) with a red diode laser at 635 nm in a multi-angle plastic cell. SEM was performed using a Philips XL30FEG scanning electron microscope with an operating voltage of 20 kV or 15 kV. An EDS detector (coupled with SEM) of similar type and brand to the one coupled with the TEM instrument, as described above, was used to analyse the elemental composition of the samples. Samples were sputter-coated with 20 nm Au films before SEM measurements.

3. Results and discussion

3.1. Preparation and characterization of FeS DSNPs

In aqueous solution, Fe^{2+} ions are complexed with PAMAM dendrimers. Upon the addition of S^{2-} anions to the Fe^{2+}–PAMAM complexes, relatively monodisperse FeS DSNPs formed, because the PAMAM branches block the overgrowth and aggregation of FeS NPs. Three different G4 PAMAMs with amine, hydroxyl, and carboxyl termini were used as stabilizers to prepare different FeS DSNPs. UV–vis spectrometry, TEM, SAED, and EDS were used to characterize these FeS DSNPs.

Figure 1 shows the UV–vis spectra of {FeS–G4·NH$_2$}, {FeS–G4·NGlyOH}, and {FeS–G4·SAH} DSNPs in aqueous solution with different concentrations of FeS. For {FeS–G4·NH$_2$} DSNPs (figure 1(a)), in the absence of the inorganic sulfide, PAMAM dendrimers have no prominent absorbance at 250–1000 nm because of the aliphatic nature of their molecular backbones [19]. In contrast, in the presence of FeS NPs, a strong buildup in absorption at 250–1000 nm can be observed in the spectra, indicating the formation of FeS DSNPs. The absorption peak at 630 nm may be attributable to the surface plasmon resonance of FeS NPs. With the increase of FeS NP concentration, the absorption in the wavelength range 250–1000 nm increases. Likewise, the plasmon peak at 630 nm also becomes more and more profound, suggesting a closer interparticle distance and a stronger interparticle interaction.

Using a hydroxyl-terminated G4·NGlyOH dendrimer, FeS NPs have also been synthesized. Clearly, in the absence of FeS NPs, G4·NGlyOH has no obvious absorbance in the 250–1000 nm range (figure 1(b)). However, after the formation of FeS NPs, a prominent broad band developed at 250–1000 nm. With the increase in the FeS NP concentration, the intensity of the broad band as well as of the surface plasmon resonance band at 610 nm also increases (figure 1(b)). These results are quite similar to those of {FeS–G4·NH$_2$} DSNPs.

The UV–vis spectra of {FeS–G4·SAH} DSNPs are quite different from those of {FeS–G4·NH$_2$} and {FeS–G4·NGlyOH} DSNPs (figure 1(c)). The absorbance profile of {FeS–G4·SAH} DSNPs is quite similar to the G4·SAH dendrimer stabilizers at low FeS concentration range (2.3–4.7 × 10^{-4} M). When the
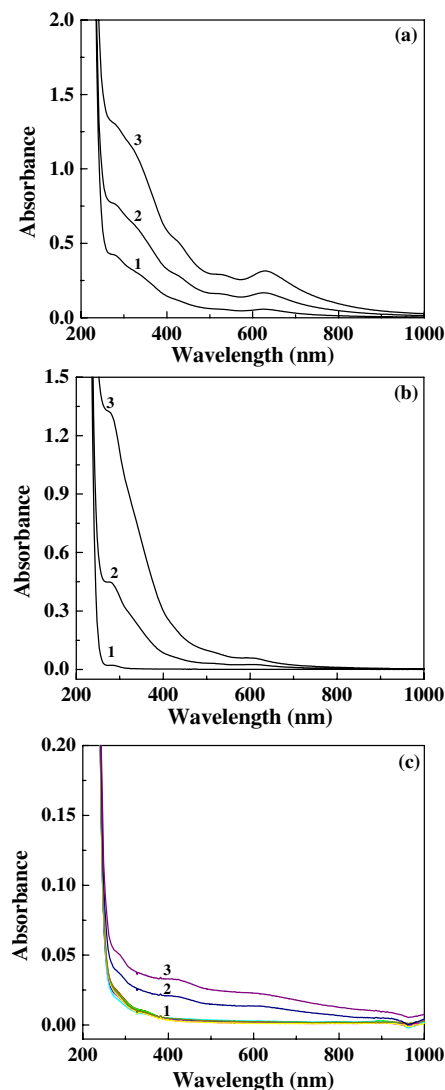
Figure 1. UV–vis spectra of {FeS–G4·NH$_2$} (a), {FeS–G4·NGlyOH} (b), and {FeS–G4·SAH} (c) DSNPs with different concentrations of FeS NPs prepared using FeCl$_2$ salt. For (a), 1, 2, and 3 represent 9.1 × 10^{-5} M, 1.7 × 10^{-4} M, and 2.8 × 10^{-4} M, respectively. For (b), 1, 2, and 3 represent 0 M, 9.1 × 10^{-5} M, and 2.8 × 10^{-4} M, respectively. For (c), 1, 2, and 3 represent a range between 2.3–4.7 × 10^{-4} M, 5 × 10^{-4} M, and 5.2 × 10^{-4} M, respectively.

(This figure is in colour only in the electronic version)

FeS concentration is increased up to 5 × 10^{-4} M, a broad band profile can be observed at 250–1000 nm. It should be noted that iron sulfides may have different chemical compositions, depending on preparation conditions such as the pH, local environment (i.e. dendrimer surface groups), the presence of ions, and so forth. These factors, and the sensitivity of FeS NPs to oxidation, make exact identification of the species in the UV–vis spectra difficult.

The as-prepared FeS DSNPs are quite stable under anaerobic conditions. UV–vis spectra of FeS DSNP solutions in sealed vials were monitored periodically for up to 2 months without displaying significant changes in the absorbance. The solutions remained transparent and no particle sedimentation occurred. In contrast, in the absence of PAMAMs, FeS
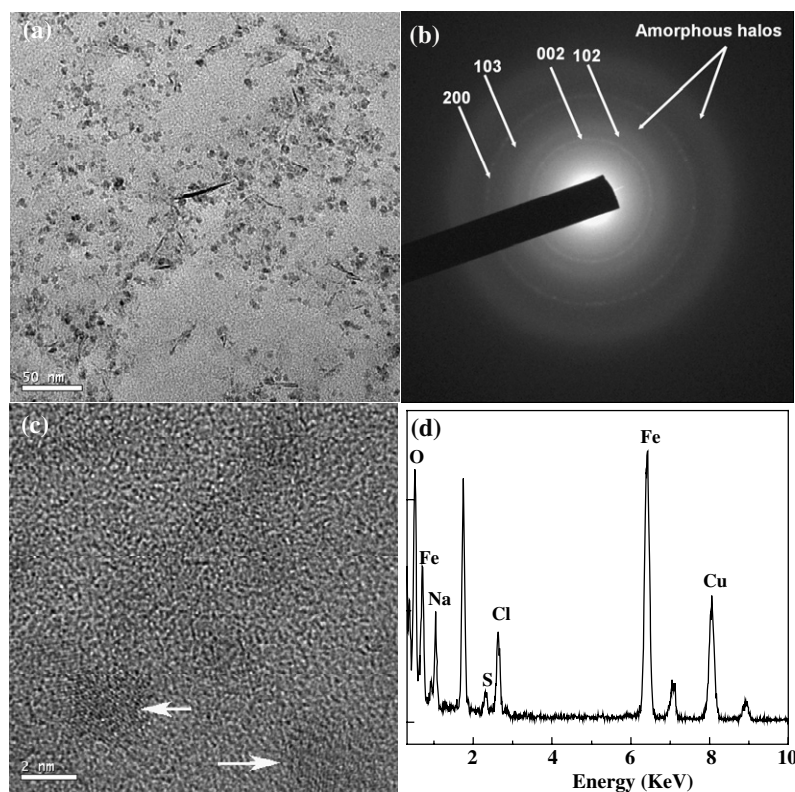
Figure 2. TEM results of {FeS–G4·NH$_2$} DSNPs prepared using FeCl$_2$ salt: (a) low-magnification TEM image; (b) SAED pattern; (c) high-resolution TEM image showing individual FeS DSNPs; (d) EDS spectrum of {FeS–G4·NH$_2$} DSNPs.

Table 1. Zeta-potential values of FeS DSNPs.

DSNPs	PS std[a]	{FeS–G4·NH$_2$}[b]	{FeS–G4·NH$_2$}[c]	{FeS–G4·NGlyOH}[c]	{FeS–G4·SAH}[c]
Zeta potential (mV)	−42.41	12.09	12.01	5.17	−7.80

[a] Standard polystyrene nanoparticles with negative zeta potential (−40–45 mV).
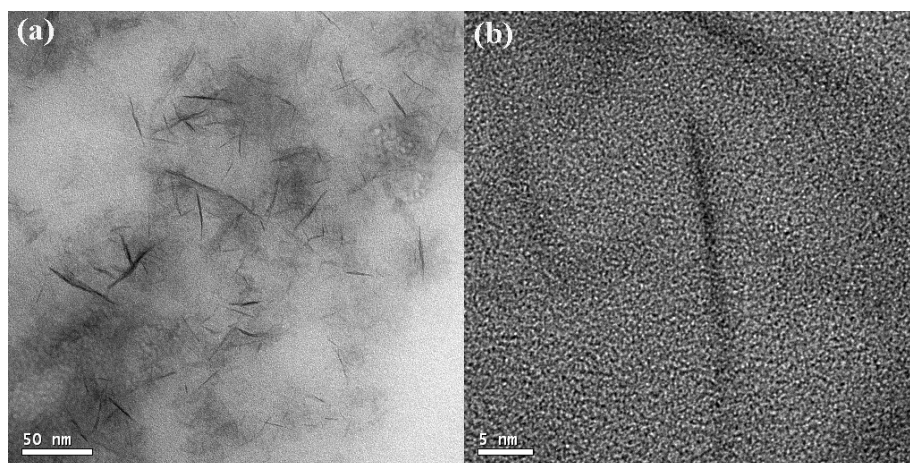
[b] Prepared using Fe(NH$_4$)$_2$(SO$_4$)$_2$ salt.

[c] Prepared using FeCl$_2$ salt.

colloids prepared under the same conditions precipitated quickly within several hours. We also compared the UV–vis spectra of the FeS DSNP samples stored in 2 ml ampoules over an even longer time—up to 5 months. It appears that {FeS–G4·NGlyOH} DSNPs are stable under different conditions (including dark at both room temperature and 4 °C, and bright at both room temperature and 4 °C), while {FeS–G4·SAH} and {FeS–G4·NH$_2$} are not stable at room temperature for up to 5 months. In any case, all FeS DSNPs are not sensitive to light, but rather to temperature.

The surface potentials of FeS DSNPs were determined by zeta-potential measurements. Table 1 lists the measured zeta-potential values of FeS DSNPs in aqueous solutions. All FeS DSNPs display the same polarity as those of the PAMAM stabilizers. For {FeS–G4·NH$_2$} DSNPs prepared using different iron (II) salts, the zeta-potential values are fairly similar, but the morphologies are significantly different, as demonstrated by TEM (see below).

Figure 2 shows the TEM images of {FeS–G4·NH$_2$} DSNPs prepared using FeCl$_2$ as the iron (II) salt. It is clear that the particles formed are predominantly presented as a spherical shape (diameter 4–6 nm). Only a small portion of needle-shaped NPs are presented in the TEM images (figure 2(a)). An SAED pattern (figure 2(b)) taken from the same area of these NPs shows dotted ring features, indicating that the {FeS–G4·NH$_2$} NPs formed are in a crystalline phase, which is in agreement with the literature [32]. The SAED pattern (figure 2(b)) shows that the crystal structure of FeS is hexagonal, with a space group of $P6_3/mmc$ ($a = 0.3452$ nm, $c = 0.5762$ nm). A high-resolution TEM image (figure 2(c)) shows that most of the NPs are polycrystalline. Through analysis of the EDS spectra, the composition of the {FeS–G4·NH$_2$} DSNPs has been identified (figure 2(d)). The low signal of the sulfur element is probably due to the oxidation of FeS in air during TEM sample preparation. It is interesting to note that the morphology of {FeS–G4·NH$_2$} DSNPs can be tuned by varying iron (II) salts with different anions. In contrast with the predominant round-shaped {FeS–G4·NH$_2$} DSNPs prepared using FeCl$_2$ salt, when Fe(NH$_4$)$_2$(SO$_4$)$_2$ was used to prepare the FeS DSNPs under similar conditions, the particles formed display a needle-like shape with a length of 15–32 nm and a diameter of about 2 nm (figure 3(a)); a high-resolution TEM image (figure 3(b)) also shows individual

Figure 3. TEM images of {FeS–G4·NH$_2$} DSNPs prepared using Fe(NH$_4$)$_2$(SO$_4$)$_2$ salt: (a) low-magnification TEM image; (b) high-resolution TEM image showing individual needle-shaped FeS DSNPs.

Table 2. Zeta-potential values of silica gel particles before and after loading with {FeS–G4·NH$_2$} DSNPs.

| Materials	PS std[a]	SiO$_2$	{FeS–G4·NH$_2$}	SiO$_2$/{FeS–G4·NH$_2$}
Zeta potential (mV)	−44.84	−14.57	12.01	11.73

[a] Standard polystyrene nanoparticles with negative zeta potential (−40–45 mV).

needle-shaped FeS DSNPs and the crystallites of the particles are rather weak compared to those prepared using FeCl$_2$.

3.2. Loading FeS NPs onto mesoporous silica gel microparticles

To manipulate FeS DSNPs as a useful formulation for environmental applications, it is necessary to deposit FeS NPs onto microparticle carriers [33, 34]. In this study, we attempted to load FeS DSNPs onto mesoporous silica gel microparticles using two approaches: approach (A), direct coating of {FeS–G4·NH$_2$} DSNPs onto silica microparticles through electrostatic assembly; and approach (B), using G4·NH$_2$-coated silica particles to incorporate Fe^{2+} ions for subsequent formation of FeS NPs. For approach (A) to verify the loading of FeS DSNPs onto silica gel microparticles, we monitored the change of surface potential of slica microparticles before and after loading with the {FeS–G4·NH$_2$} DSNPs. It is clear that the negative surface potential of the silica gel particles reverses to positive after loading with {FeS–G4·NH$_2$} DSNPs (table 2). The surface charge reversal of silica gel particles demonstrates the effective loading of {FeS–G4·NH$_2$} DSNPs. SEM images show the morphology changes after coating of {FeS–G4·NH$_2$} DSNPs onto silica gel microparticles (figure 4). The surface of the silica particles appears much rougher than that of the uncoated silica particles. However, EDS analysis cannot differentiate the existence of FeS signals after coating with the {FeS–G4·NH$_2$} DSNPs, indicating that the loading percentage of {FeS–G4·NH$_2$} DSNPs is lower than 1%, which is up to the EDS detection limit.

In order to increase the incorporation of FeS NPs, approach (B) was performed. It is well known that amine-terminated PAMAM dendrimers can be easily adsorbed onto mesoporous silica microparticles [35]. The dendrimer
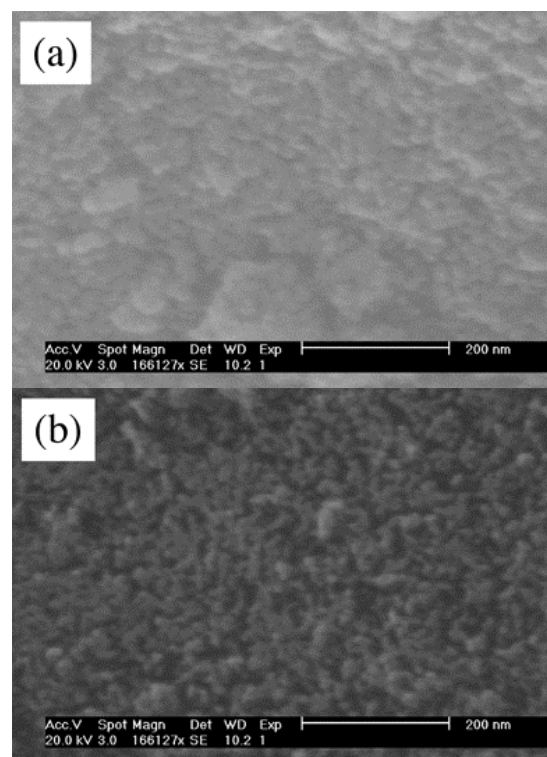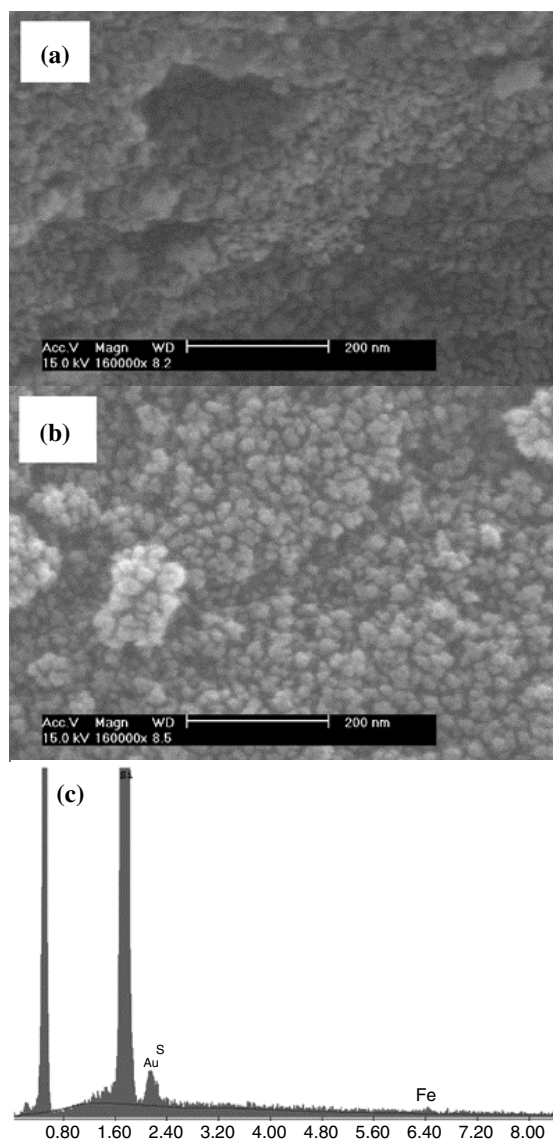

Figure 4. SEM images of a silica gel particle before (a) and after (b) coating with {FeS–G4·NH$_2$} DSNPs using approach (A).

monolayer adsorbed onto silica microparticles was used as a nanoreactor for subsequent complexation with Fe^{2+} ions and the formation of FeS NPs. In this case, much more FeS NPs have been loaded onto silica particles. The EDS spectrum (figure 5(c)) clearly shows the presence of Fe and

Table 3. Zeta-potential values of silica particles in each step coating.

Materials	PS std[a]	SiO$_2$	SiO$_2$/G4·NH$_2$	SiO$_2$/G4·NH$_2$/Fe^{2+}	SiO$_2$/G4·NH$_2$/FeS
Zeta potential (mV)	−42.05	−14.57	33.46	29.34	0.55

[a] Standard polystyrene nanoparticles with negative zeta potential (−40–45 mV).

Figure 5. SEM images of a silica gel particle after coating with G4·NH$_2$ dendrimer (a) and FeS NPs (b) using approach (B). The EDS spectrum (c) of silica microparticles loaded with FeS NPs is also shown.

S elements (S peaks overlapped with Au peaks). SEM morphology studies (figures 5(a) and (b)) show that, after the formation of FeS NPs onto silica microparticles, the surface of the silica particles appears much rougher than the surface of those without FeS NP formation. We also attempted to use TEM for further characterization of the FeS DSNP loading onto silica microparticles. However, the size of the silica microparticles is approximately 40–63 μm, which makes the direct TEM imaging difficult because the sample thickness

is too big. Therefore, we think SEM is one of the best techniques for the characterization of the loading of NPs onto microparticles with sizes larger than 20 μm [36]. Further zeta-potential measurements (table 3) monitored each step of the coating of FeS NPs onto silica particles. We note that, after the formation of FeS NPs using approach (B), the zeta potential of the silica particles is close to neutral (0.55 mV), which is very different from that of FeS DSNP-coated silica particles (approach (A)). It is inferred that overgrowth of FeS NPs occurs in approach (B), because the pancake-shaped dendrimer monolayer [37, 38] on silica microparticle surfaces may not significantly limit the overgrowth of the FeS NPs compared with dendrimer molecules in solution. It is also worthwhile noting that, for the loading of FeS NPs using both approaches, both the internal pore wall surfaces and the silica microparticle surfaces may be coated with FeS NPs, because the diameter of the pores of the mesoporous silica is 6 nm, which is large enough for the coating of FeS NPs (4–6 nm in diameter). In order to further control and manipulate the loading capacity of FeS NPs onto silica microparticle surfaces, PAMAM multilayers will be self-assembled onto silica particles using an oppositely charged linear polymer (e.g. polystyrene sulfonate sodium salt) in an LbL manner. The PAMAM multilayers coated on silica microparticles will be used as nanoreactors to complex with Fe^{2+} ions for subsequent FeS NP formation. In this case, the loading capacity of FeS NPs can be controlled by varying the thickness of PAMAM multilayers and the number of reaction cycles for the formation of FeS NPs. The morphologies and distribution of FeS NPs embedded into PAMAM/PSS multilayers will be further investigated using planar substrates as a model system. This work is currently ongoing in our lab.

4. Conclusion

In summary, FeS DSNPs have been successfully synthesized using G4·NH$_2$, G4·NGlyOH, and G4·SAH, respectively, as stabilizers. Deposition of FeS NPs onto mesoporous silica gel microparticles was confirmed by zeta-potential and SEM measurements. We show that dendrimer-coated silica particles facilitate the much more effective loading of FeS NPs. The synthesis and manipulation of FeS NPs onto mesoporous silica microparticles provide versatile platforms for their environmental remediation applications.

Acknowledgments

References

[1] Zhang W X and Masciangioli T 2003 *Environ. Sci. Technol.* **37** 102A

[2] Butler E C and Hayes K F 2000 *Environ. Sci. Technol.* **34** 422

[3] Chin P P, Ding J, Yi J B and Liu B H 2005 *J. Alloys Compounds* **390** 255

[4] Watson J H P, Croudace I W, Warwick P E, James P A B, Charnock J M and Ellwood D C 2001 *Separation Sci. Technol.* **36** 2571

[5] Watson J H P, Cressey B A, Roberts A P, Ellwood D C, Charnock J M and Soper A K 2000 *J. Magn. Magn. Mater.* **214** 13

[6] Watson J H P, Ellwood D C, Soper A K and Charnock J 1999 *J. Magn. Magn. Mater.* **203** 69

[7] Bi X X and Eklund P C 1993 *Mater. Res. Soc. Symp. Proc.* **286** 161

[8] Chadha A, Sharma R K, Stinespring C D and Dadyburjor D B 1996 *Ind. Eng. Chem. Res.* **35** 2916

[9] Wilcoxon J P, Newcomer P P and Samara G A 1996 *Solid State Commun.* **98** 581

[10] Paknikar K M, Nagpal V, Pethkar A V and Rajwade J M 2005 *Sci. Technol. Adv. Mater.* **6** 370

[11] Zheng J, Stevenson M S, Hikida R S and Van Patten P G 2002 *J. Phys. Chem.* **106** 1252

[12] Zheng J, Petty J T and Dickson R M 2003 *J. Am. Chem. Soc.* **125** 7780

[13] Zheng J, Zhang C and Dickson R M 2004 *Phys. Rev. Lett.* **93** 077402/1

[14] Zhao M, Sun L and Crooks R M 1998 *J. Am. Chem. Soc.* **120** 4877

[15] Balogh L and Tomalia D A 1998 *J. Am. Chem. Soc.* **120** 7355

[16] Crooks R M, Zhao M, Sun L, Chechik V and Yeung L K 2001 *Acc. Chem. Res.* **34** 181

[17] Esumi K, Suzuki A, Aihara N, Usui K and Torigoe K 1998 *Langmuir* **14** 3157

[18] Grohn F, Bauer B J, Akpalu Y A, Jackson C L and Amis E J 2000 *Macromolecules* **33** 6042

[19] Shi X, Ganser T R, Sun K, Balogh L P and Baker J R Jr 2006 *Nanotechnology* **17** 1072

[20] Tomalia D A and Frechet J M J 2001 *Dendrimers and Other Dendritic Polymers* (New York: Wiley)

[21] Tan N C B, Balogh L, Trevino S F, Tomalia D A and Lin J S 1999 *Polymer* **40** 2537

[22] Sooklal K, Hanus L H, Ploehn H J and Murphy C J 1998 *Adv. Mater.* **10** 1083

[23] Lemon B I and Crooks R M 2000 *J. Am. Chem. Soc.* **122** 12886

[24] Oh S-K, Kim Y-G, Ye H and Crooks R M 2003 *Langmuir* **19** 10420

[25] Knecht M R, Garcia-Martinez J C and Crooks R M 2005 *Langmuir* **21** 11981

[26] Lesniak W, Bielinska A U, Sun K, Janczak K W, Shi X, Baker J R Jr and Balogh L P 2005 *Nano Lett.* **5** 2123

[27] Decher G 1997 *Science* **277** 1232

[28] Donath E, Sukhorukow G B, Caruso F, Davis S A and Moehwald H 1998 *Angew. Chem Int. Edn* **37** 2201

[29] Caruso F, Caruso R A and Mohwald H 1998 *Science* **282** 1111

[30] Shi X, Shen M and Moehwald H 2004 *Prog. Polym. Sci.* **29** 987

[31] Shi X, Lesniak W, Islam M T, Muñiz M C, Balogh L and Baker J R Jr 2006 *Colloids Surf.* A **272** 139

[32] Daams J L C, Villars P and van Vucht J H N 1991 *Atlas of Crystal Structure Types for Intermetallic Phases* (Newbury: ASM International)

[33] Dekany I, Turi L, Homonnay Z, Vertes A and Burger K 1996 *Colloids Surf.* A **119** 195

[34] Dekany I, Turi L, Vanko G, Juhasz G, Vertes A and Burger K 1996 *NATO ASI Series, Series 3: High Technology* vol 18, p 555

[35] Ottaviani M F, Turro N J, Jockusch S and Tomalia D A 2003 *J. Phys. Chem.* B **107** 2046

[36] Kidambi S, Dai J, Li J and Bruening M L 2004 *J. Am. Chem. Soc.* **126** 2658

[37] Imae T, Funayama K, Aoi K, Tsutsumiuchi K, Okada M and Furusaka M 1999 *Langmuir* **15** 4076

[38] Bosman A W, Janssen H M and Meijer E W 1999 *Chem. Rev.* **99** 1665